Robotics and Autonomous Systems 63 (2015) 57–67

Contents lists available at ScienceDirect

Robotics and Autonomous Systems

journal homepage: www.elsevier.com/locate/robot

8-DoF biped robot with compliant-links

Abhishek Sarkar *, Ashish Dutta

IIT Kanpur, 208016, India

HIGHLIGHTS

- New design of an 8-DoF biped robot with compliant links for walking.
- Compliant links of different thickness are used and corresponding work done is found.
- Dynamic equation of the biped is derived using the Lagrange–Euler method to find the work done.
- Genetic algorithm is used to find the optimal gait, with constraints that satisfy ZMP.
- Both simulation and experiments are performed with the designed compliant biped.

ARTICLE INFO

Article history:
Received 24 January 2014
Received in revised form
27 August 2014
Accepted 1 September 2014
Available online 2 October 2014

Keywords:
Flexible-link planar biped
Walking gait
Pseudo-rigid body model
Optimization

ABSTRACT

This paper proposes a new design of an 8-degree of freedom (DoF) biped robot with compliant links and its optimum trajectory generation for walking. The shanks of a biped are replaced by compliant links. Compliant links of different thickness are used to find optimum walking trajectory and the work done is compared for different cases. Compliant links are modelled using the pseudo-rigid body model (PRBM), in which a single compliant link is divided into two rigid links connected by a pin joint and a torsional spring at the joint. Gait trajectory is generated for continuous walking by defining the hip and swing foot ankle trajectories with respect to the stance-leg ankle. Different constraint conditions are taken into consideration to ensure continuity and smoothness of the walking trajectory in a straight path. The dynamic equations of motion of the bipeds are derived using the Euler–Lagrangian method and the work done for both rigid and compliant biped are obtained. The genetic algorithm (GA) is used to optimize the trajectory to minimize the work done. For dynamic balance of the biped, the zero-moment point (ZMP) method is used. By varying the thickness of compliant link and other gait parameters, various gait trajectories are simulated and compared based on the work done and balance. Experiments were carried out in which a biped robot with compliant links was made to follow the optimal trajectories and the experimental results are compared with simulation results.

1. Introduction

Biped robots have been studied by several researchers due to their advantages in locomotion over wheeled mobile robots. Though much research has been done in the area of dynamic biped gait generation [1–3], a stable human-like dynamic walk [4–6], has not been achieved [7]. Biped robots have many degrees of freedom and hence the focus of several past studies has been in trying to implement non-actuated joints by adding springs at the sole of feet, joints or links [8,9]. Adding compliance can be done at different levels, i.e. attaching torsional springs in the actuated joints [9], compliant ankle joint [10], designing compliant leg with linear spring mechanism [11,12] to reduce re-bouncing of the feet off the ground. The compliant leg is also found advantageous for running and jumping like locomotions [11]. Deformable feet design is found adaptable to perturbation and change in walking speed [13]. There are also biped models which are actuated with linear artificial muscles [14,15].

The objectives of this paper are listed as:

(1) Design a biped robot with compliant shanks.
(2) Develop an optimal continuous gait pattern for the compliant biped to walk in a horizontal straight path.
(3) Simulation and experimental evaluation of the biped.

The generation of gait trajectory is discussed in Section 2 and the inverse kinematics for finding the joint angles is calculated in Section 3. Dynamic equations for both rigid-link and compliant-link bipeds are derived using Euler–Lagrangian method (Section 4),

* Corresponding author. Tel.: +91 9628560050.
E-mail addresses: abhisar@iitk.ac.in, abhi.romi@gmail.com (A. Sarkar), adutta@iitk.ac.in (A. Dutta).

http://dx.doi.org/10.1016/j.robot.2014.09.014
0921-8890/

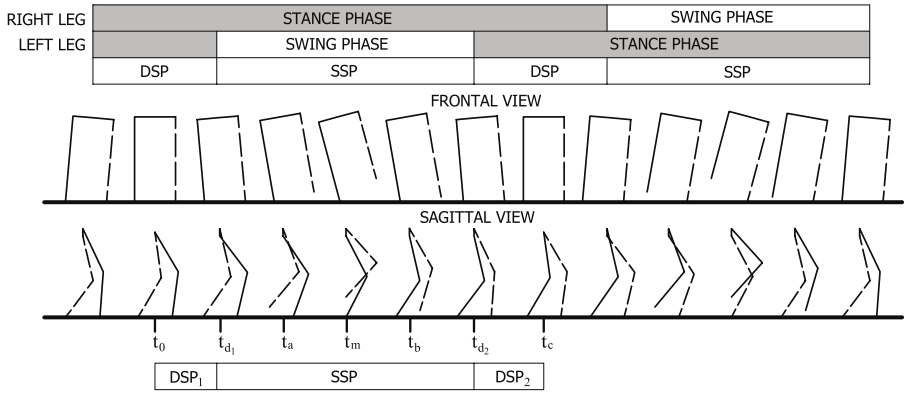

Fig. 1. Frontal and sagittal views of a complete walking cycle of a biped gait.

to calculate joint torques and work done. A biped is designed in which the shanks of an 8-DoF biped are replaced with compliant 'C'-shaped links. The details of design of the compliant biped is discussed in Section 5. The deflection in the compliant links during walking cycle due to the force and moment acting on the compliant link is calculated using PRBM [16,17]. In PRBM a single compliant link is replaced by two rigid links connected by a pin joint with a torsion spring at the joint. The deflection of the compliant section was computed based on the forces and moments acting at the knee joint. Simulations are done by varying the hip and leg trajectory and GA is used to find the optimum trajectory for continuous walk. Simulation and experimental results are shown in Section 6 and in Section 7 conclusion of the work is presented.

2. Walking pattern generation

Human locomotion can be divided into three types namely walking, jumping and running. Many researchers tried to reproduce these locomotion strategies by using different specialized designs of biped. It is found that designing a walking robot with stiff rigid links is sufficient for walking [1]. Jumping or running bipeds are designed with springs and dampeners for more shock-absorbing capabilities [8,11,13]. Also researchers argued in favour of compliant legs for the walking gait [11]. In this work we propose a biped robot with lightweight compliant shanks for walking.

Natural human walking gait is biphasic, and bilaterally symmetric (Fig. 1). Generally a cycle of a biped walking pattern is considered to start with a heel strike (foot placement) and end with another heel strike of the same leg. In this study for simplicity we considered that the feet always remain horizontal. The two phases of human walking cycle are stance phase and swing phase. Based on the combinations of these stance and swing of both legs the walking cycle is divided into single supported phase (SSP) where only one foot is in stance and double supported phase (DSP), where both feet are in stance.

For simulation we considered the beginning of the step (t_0) from the mid-DSP and the ending (t_c) is next mid-DSP. So, t_0 to t_{d_1} is called as DSP_1 and t_{d_2} to t_c is DSP_2. At the bottom of the figure the part taken for the simulation step is shown. The right leg in one step behaves as the left leg in the next step and vice versa. Thus the joint angles of the right leg in a step will be the same as the joint angles of the left leg in the previous step,

$$\theta_{right}(t) = \theta_{left}(t - t_c) \tag{1}$$

where t_c is the step time and θ_{right} and θ_{left} are the vectors of leg joint angles, $[\theta_{hip}, \theta_{knee}, \theta_{ankle\ roll}, \theta_{ankle\ pitch}]^T$ for the corresponding legs. Thus the whole walking pattern can be generated by repetition of left and right step consecutively.

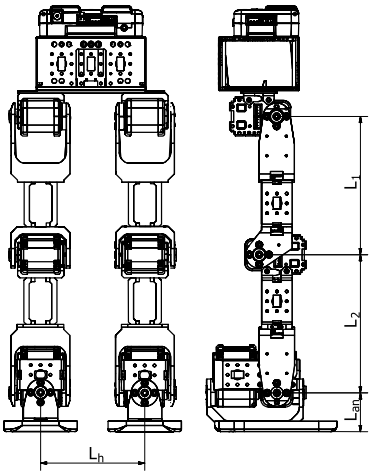

Fig. 2. CAD model of Bioloid biped.

Table 1
Specifications of rigid-link biped robot.

Link	Length (m)
Thigh (L_1)	0.111
Shank (L_2)	0.111
Hip link (L_h)	0.085
Ankle-joint height (L_{an})	0.032

Simulation step time, t_c, is divided into 50 time points. Each of the DSPs consists of 10 divisions (i.e. $0.2t_c$), so $t_{d_1} = 0.2t_c$ and $t_{d_2} = 0.8t_c$. The time t_a, t_b and t_m are intermediate time points used to generate spline trajectory of swing-leg ankle [where, $t_m = t_c/2$, $t_a = (t_{d_1} + t_m)/2$ and $t_b = (t_m + t_{d_2})/2$].

3. Kinematics of biped

First an 8-DoF Biped robot with rigid links is analysed and then its shank links are replaced with compliant links below the knee joint. The biped model has 8-DoF made with Bioloid [18] Premium kit (Fig. 2). It has a lower trunk, and both legs have thigh, shank and foot (feet are made with two links). Hip and knee joints of both legs have pitch motions, and both ankles have roll and pitch motion. The link lengths of the biped robot are given in Table 1. The length and width of each foot are 0.1 m and 0.06 m respectively.

The coordinate-frame assignment of the rigid-link biped is shown in Fig. 3. The global coordinate frame is denoted by '**G**'. The biped base coordinate-frame, '**0**' is denoted at the toe of the stance foot. Coordinate frame number '**1**'–'**8**' are assigned for the 8-actuated joints of the rigid biped starting from the stance-leg

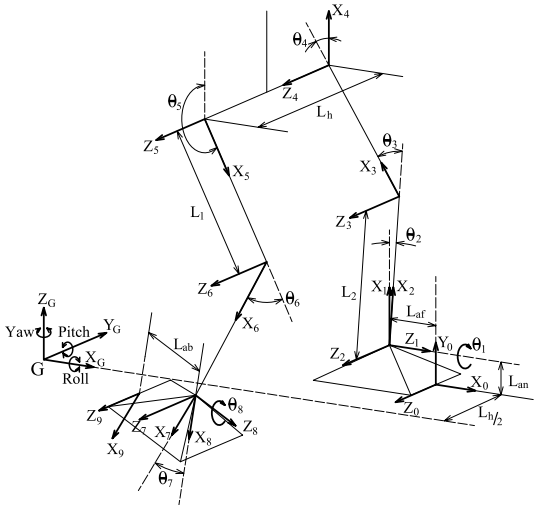

Fig. 3. Rigid-link biped coordinate frames assignment.

Table 2
CoM of the links of the rigid biped robot.

Coordinate-frame $(i-1)$	m_i (g)	r_{ix} (mm)	r_{iy} (mm)	r_{iz} (mm)
0	35.6	−55.4	5.9	0
1	159.0	17.4	0	−15.4
2	79.4	63.5	0	0
3	29.6	33.9	0	0
4	344.4	32.6	26.2	32.0
5	29.6	41.0	0	0
6	79.4	11.5	0	0
7	159.0	−17.4	−15.4	0
8	35.6	26.0	0	−5.7

Table 3
DH parameters for rigid-link biped.

Link i	θ_i	α_i	a_i	d_i
1	θ_1	$-\pi/2$	0	0
2	θ_2	0	L_1	0
3	θ_3	0	L_2	0
4	θ_4	0	0	$-L_h$
5	θ_5	0	0	0
6	θ_6	0	L_2	0
7	θ_7	$\pi/2$	L_1	0
8	θ_8	0	0	0

ankle to the swing-leg ankle. The '**9**'th coordinate frame is assigned at the heel of the swing foot. We have not considered feet rotation with respect to the ground in this work for the biped walking pattern generation.

Coordinates of centre of mass (CoM) for link '*i*' with respect to the origin of the corresponding link coordinate-frames, O_{i-1}, are denoted by $r_i = [r_{ix}, r_{iy}, r_{iz}]$. The values of link masses, m_i and CoM coordinates, r_i for the biped robot are shown in Table 2.

The Denavit–Hartenberg (DH) parameters for the 8-DoF rigid link was assigned for the biped coordinate-frames in Table 3.

3.1. Inverse kinematics for rigid biped

The biped gait pattern is generated for walking on the flat horizontal ground in the straight path. During SSP, the whole body weight is supported and balanced by stance-leg and simultaneously it moves the lower trunk forward. The swing-leg from the hip joint swings forward during SSP and becomes the stance-leg in the next step. In the sagittal plane there are 2-DoFs between the ankle and hip joint of the stance-leg. We have defined the motion of the hip joint in the sagittal (XZ) plane by a sinusoidal curve.

Inverse kinematics of the biped is done by the graphical method [19]. Two situations arise in the inverse kinematics of rigid biped, as shown in Fig. 4(a) and (b). First when the hip joint is behind of the ankle joint (Fig. 4(a)); second when the hip joint is ahead of the ankle joint (Fig. 4(b)). The angle of the shank with the vertical direction, (θ_2), is given by,

$$\theta_2 = \begin{cases} \phi - \psi & \text{if } O_{x_4} < O_{x_2} \\ \phi + \psi & \text{if } O_{x_4} \geq O_{x_2} \end{cases} \tag{2}$$

where O_{x_i} is the X-coordinate of the origin of the '***i***'th coordinate-frame with respect to base '**G**', and from geometry we have,

$$\psi = \tan^{-1}\left(\frac{O_{x_4} - O_{x_2}}{O_{z_4} - O_{z_2}}\right) \tag{3}$$

$$\phi = \cos^{-1}\left(\frac{L_1^2 + d^2 - L_2^2}{2L_2 d}\right) \tag{4}$$

$$d = \sqrt{(O_{z_4} - O_{z_2})^2 + (O_{x_4} - O_{x_2})^2}. \tag{5}$$

If, $L_1 = L_2$, then

$$\theta_3 = 2\phi \tag{6}$$

$$\theta_4 = \theta_3 - \theta_2. \tag{7}$$

In our model, the link lengths are equal, $L_1 = L_2$, and the joint angles are calculated from the above equations. The hip joint angle θ_4 is found from the condition that the lower trunk is always vertical in the sagittal plane. Similarly, the joint angles for the swing-leg (θ_5, θ_6 and θ_7) are also calculated. The swing-leg ankle trajectory is defined by a spline curve and swing foot is always assumed to be horizontal (parallel to the ground). In the frontal (YZ) plane there are 2-DoFs, from the roll DoFs of both the ankles. The side tilt angle of the biped is given as input by $\theta_1(t)$, and $\theta_8(t) = -\theta_1(t)$.

3.2. Inverse kinematics for compliant biped

For compliant biped two more coordinate-frames are included due to the PRBM of compliant links of both legs as discussed in Section 5. The compliant link is divided into two rigid links connected by a pin joint as PRBM. The PRBM link joints are situated between the ankle joint and knee joint of both legs and corresponding joint numbers become '3' and '8'. So, the total number of joints including two compliant joint become 10. After calculating the angles of deflection in compliant links (θ_3 and θ_8), for the rest of the angles the inverse kinematics is done with the graphical method.

Again, for the compliant biped two situations arise similar to the rigid biped case (Fig. 5(a) and (b)). The link lengths from the pseudo-link joint to the knee joint and ankle joint are, L_t and L_b, respectively. The effective length of the shank, '*e*', varies with the deflection in the compliant link. Initial undeflected length of '*e*' is $L_t + L_b = 114$ mm. So, from the geometry it can be written as,

$$e = L_b \cos(\beta) + L_t \cos(\theta_3 - \beta) \tag{8}$$

$$L_b \sin(\beta) = L_t \sin(\theta_3 - \beta). \tag{9}$$

From the above two Eqs. (8), (9), the values of '*e*' and angle 'β' are derived. Similarly, for ankle to hip-joint distances and link lengths,

$$d = e\cos(\phi) + L_1 \cos(\theta_4 - \phi) \tag{10}$$

$$e\sin(\phi) = L_1 \sin(\theta_4 - \phi). \tag{11}$$

From Eqs. (10) and (11) values of d and ϕ can be derived. The value of ψ is calculated from Fig. 5. Now, for the two cases θ_2 can be written as,

$$\theta_2 = \begin{cases} \beta - (\phi - \psi) & \text{if } O_{x_5} < O_{x_2} \\ \beta - (\phi + \psi) & \text{if } O_{x_5} \geq O_{x_2}. \end{cases} \tag{12}$$

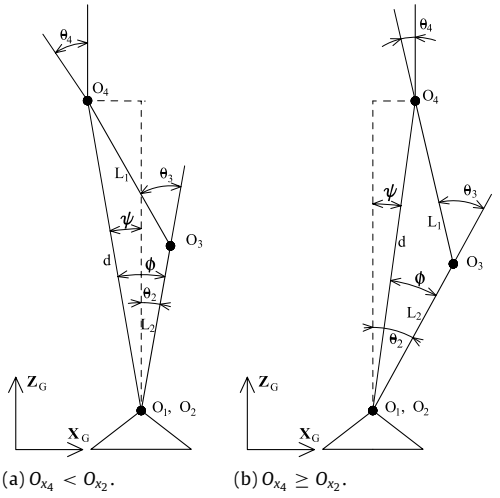

Fig. 4. Inverse kinematics of stance-leg of rigid biped in the sagittal plane in the graphical method.

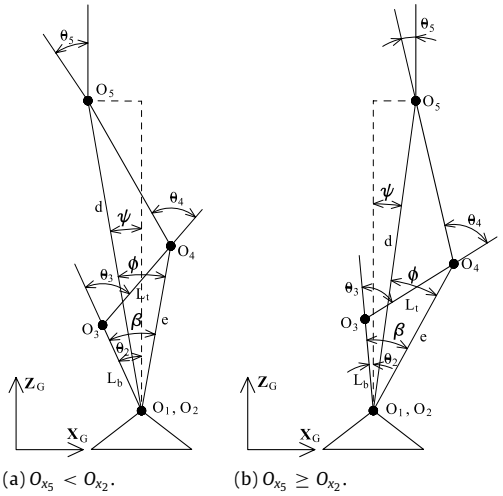

Fig. 5. Inverse kinematics of stance-leg of compliant biped (PRBM) in the sagittal plane in the graphical method.

The knee angle θ_4 is calculated from Eq. (11). Similarly, the joint angles for the swing-leg (θ_6, θ_7 and θ_9) are also calculated. The lower trunk is assumed vertical to calculate θ_5 and the swing foot is assumed parallel to the ground to calculate θ_7. The side-tilt angle of the compliant biped is given as input by $\theta_1(t)$, and $\theta_{10}(t) = -\theta_1(t)$.

3.3. Constraints

Due to mechanical design of the biped robot, the upper and lower joint angle limits, $\theta_{i_{\min}}$ and $\theta_{i_{\max}}$ respectively, are shown in Table 4.

During DSP_1 and DSP_2, both the feet stay on the ground,

$$\begin{aligned} &O_{Z_9}(t_{d_1}) = O_{Z_9}(t_{d_2}) = 0, \quad \text{for rigid biped} \\ &O_{Z_{11}}(t_{d_1}) = O_{Z_{11}}(t_{d_2}) = 0, \quad \text{for compliant biped} \end{aligned} \tag{13}$$

where O_{Z_9} and $O_{Z_{11}}$ represent the Z-coordinates of the heel coordinate frame origin for rigid and compliant link biped respectively, with respect to the global coordinate-frame '**G**'. At the end of a step, swing foot will move forward a distance of L_{step},

$$\begin{aligned} &O_{X_9}(t_c) - O_{X_9}(t_0) = L_{step}, \quad \text{for rigid biped} \\ &O_{X_{11}}(t_c) - O_{X_{11}}(t_0) = L_{step}, \quad \text{for compliant biped.} \end{aligned} \tag{14}$$

The single spline curve is generated over the step time, $[t_0, t_c]$ for each trajectory to maintain continuity between three sub-phases. After one step, biped changes support and swing-leg becomes stance-leg and vice versa. During this transition, motor-angles of stance-legs of the current step become the corresponding angles of swing-leg in the subsequent step for symmetric gait of the biped. All the pitch rotation motors of both legs are attached in the opposite direction from one another (i.e. the horn of both the knee motors are placed laterally outward). To make the joint angles of the previous step consistent with the joint angles in the current step in simulation, some constants (c_i and c_js) are introduced with continuity constraints equations,

$$\begin{aligned} &\theta_i(t + t_c) = c_i \pm \theta_{(9-i)}(t), \quad \text{for rigid biped} \\ &\theta_j(t + t_c) = c_j \pm \theta_{(11-j)}(t), \quad \text{for compliant biped} \end{aligned} \tag{15}$$

where c_i ($i = 1, 2, \ldots, 8$) and c_j ($j = 1, 2, 4, \ldots, 7, 9, 10$) are constants. When the biped changes support after one step, the base coordinate frames are redefined from the other leg. So, to maintain the similarity between the joint trajectories these constants are introduced. Also the angular velocities of the motors at the end of the first step and the beginning of the second should be equal for opposite legs. The time derivative of the trajectories are defined for the hip and swing foot ankle and the side tilt angle. These velocity

Table 4
Joint angle limits.

Joint no.		$\theta_{i_{max}}$ (rad)	$\theta_{i_{min}}$ (rad)
Rigid	Compliant		
θ_1	θ_1	$\pi/12$	$-\pi/12$
θ_2	θ_2	0	$-\pi/2$
θ_3	θ_4	$2\pi/3$	0
θ_4	θ_5	$\pi/4$	$-\pi/2$
θ_5	θ_6	$3\pi/2$	$3\pi/4$
θ_6	θ_7	0	$-2\pi/3$
θ_7	θ_9	$\pi/2$	0
θ_8	θ_{10}	$\pi/12$	$-\pi/12$

values at the end of the first step and the beginning of the second are taken as equal.

$$\dot{\theta}_i(nt_c) = \pm\dot{\theta}_{(9-i)}((n-1)t_c), \quad (i = 1, 2, \ldots, 8), \text{ for rigid biped}$$
$$\dot{\theta}_j(nt_c) = \pm\dot{\theta}_{(11-j)}((n-1)t_c), \quad (j = 1, 2, 4, \ldots, 7, 9, 10), \text{ for compliant biped} \tag{16}$$

where n is the step number. Using these constraints a continuous biped walking gait is generated.

During DSP, when both feet are touching the ground, the hip-centre cannot go beyond a certain height, $H_z^{\max}$, that is given as,

$$H_z^{\max} = \left[\sqrt{(L_1+L_2)^2 - \left(\frac{L_{step}}{2}\right)^2}\right]\cos\theta_1 - \frac{L_h}{2}\sin\theta_1. \tag{17}$$

So, during hip trajectory generation this limit is taken into consideration.

4. Dynamics of biped

4.1. Dynamic equation of rigid-link biped

Dynamics of rigid-link biped is derived with Euler–Lagrangian method [19–21]. The standard form of the dynamic equation for rigid biped is derived,

$$D(\theta)\ddot{\theta} + B(\dot{\theta}, \theta) + G(\theta) = \tau, \tag{18}$$

where D is the 8×8 symmetric and positive-definite generalized mass matrix, the vector B regroups Coriolis and centrifugal terms, and G represents gravity terms and τ is the joint torque vector. The work done for rigid biped is calculated as,

$$\mathrm{W_R} = \sum_{i=1}^{8}\int_0^{t_c} \tau.\mathrm{d}\theta. \tag{19}$$

4.2. Dynamic equation for compliant-link biped

For calculating the dynamic equations of the compliant-link biped the effects of the compliant links are incorporated in the dynamic equation. The compliant link of the stance-leg deforms due to the force and moment acting at the knee joint of the biped. Hence, the force and moment at the knee joint of the stance-leg during a walking cycle is first calculated. The total linear momentum with respect to the stance-leg knee-frame origin, O_4 is,

$$P' = \sum_{i=4}^{9} m_i\dot{p}_i \tag{20}$$

where i denotes the link numbers above the stance-leg knee joint and p_i is the distance between the knee-frame origin and CoM of the 'i'th link. The total angular momentum of the links above knee joint, with respect to the knee-frame origin, is given by:

$$H' = \sum_{i=4}^{9} p_i \times m_i\dot{p}_i + I_i\omega_i \tag{21}$$

where i denotes the link numbers above the stance-leg knee joint, I_i is the inertia tensor and ω_i is the angular velocities of the 'i'th link, with respect to the knee frame. The compliant link is assumed to move in a plane i.e. only rotation is allowed. The pseudo-rigid body dynamic model (PRBDM) [22] is used to calculate kinetic and potential energy of the compliant link. Elastic mechanical coupling is considered between the PRBM links L_t and L_b, as a linear torsional spring with constant stiffness coefficient. The Lagrange equation is used [23] to calculate the joint torques for the compliant-link biped as:

$$\left.\begin{aligned} D(\theta)\ddot{\theta} + B(\dot{\theta}, \theta) + G(\theta) = \tau, \\ K\Delta\theta_i = 0 \end{aligned}\right\} \tag{22}$$

where i (=3 & 8) represents the two pseudo rigid body joints. $K = \mathrm{diag}[K_1, K_2]$, $(K_1 = K_2)$ is a diagonal stiffness matrix which models the joint elasticity of the PRBM joints. As the PRBM joints are not actuated, so the external input torques are zero in the second equation.

The work done for compliant biped is calculated as,

$$\mathrm{W_C} = \sum_{\substack{j=1 \\ j\neq 3\ \&\ 8}}^{10}\int_0^{t_c} \tau.\mathrm{d}\theta, \quad \text{for compliant biped.} \tag{23}$$

For the compliant biped no work is done for joints 3 and 8 as they are the passive joints.

4.3. ZMP balance

The concept of ZMP [24,25] is used in gait planning for biped robot and its control as a criterion of postural stability. The distance of CoM with respect to the base frame is denoted as, $P_{CoM} = [x_{CoM}, y_{CoM}, z_{CoM}]^T$. H and P are angular and linear momentum with respect to the base frame origin and g is the acceleration due to gravity. The distance from base frame origin to the location of ZMP, $p_{ZMP} = [x_{ZMP}, y_{ZMP}, z_{ZMP}]$, can be computed as,

$$x_{ZMP} = \frac{m_{tot}gx_{CoM} + z_{ZMP}\dot{P}_x - \dot{H}_y}{m_{tot}g + \dot{P}_z}$$
$$y_{ZMP} = \frac{m_{tot}gy_{CoM} + z_{ZMP}\dot{P}_y - \dot{H}_x}{m_{tot}g + \dot{P}_z} \tag{24}$$

where $m_{tot} = \sum_{i=1}^{9} m_i$ is the total mass of the biped, z_{ZMP} is the height of the floor. As the XY-plane of the base frame '**G**' is on the floor, so $z_{ZMP} = 0$.

5. Compliant link design

The compliant biped has been designed by using a 'C'-shaped compliant link and attached just below the knee joint as shown in Fig. 6. This shape has been chosen as it provides maximum deflection and no stress-concentration due to bending. The compliant links for simulation are made of aluminium, with different thicknesses (0.5, 1, 1.5 and 2 mm), 26 mm width and effective length, l_c = 38 mm. The undeflected length of the compliant link plus the length of rigid connectors to attach with the knee and ankle motors is taken same as the length, L_2 of the shank of rigid biped. The length from the knee joint to the top of the compliant link is l_t (=19 mm) and the length from the ankle joint to the bottom of the compliant link is l_b (=55 mm). So, the total length from the pseudo-link joint to knee joint is $L_t = (\gamma l_c + l_t)$ and length from the pseudo-link joint to ankle joint is $L_b = ((1-\gamma)l_c + l_b)$, where γ is the characteristics radius factor of PRBM.

5.1. Pseudo-rigid-body model

PRBM is a simplified method for kinematic design of compliant mechanism based on static and kinematic analysis [16,17,26]. It provides an easy means for large-deflection, non-linear analysis.

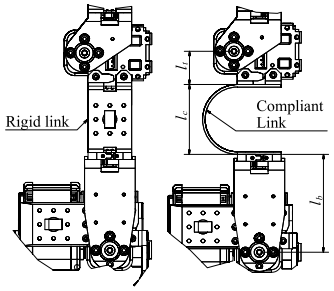

Fig. 6. Shank of the rigid biped (left) is replaced with compliant link (right).

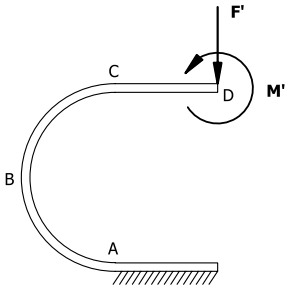

Fig. 7. The 'C'-shaped compliant link subjected to end-force and moment.

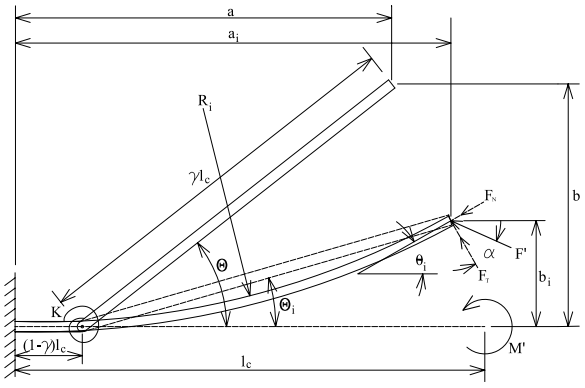

Fig. 8. Compliant beam and corresponding PRBM due to moment and force load.

PRBM is the simple numerical approximation for complex elliptical integral for beam bending equations. The 'C'-shaped beam is subjected to a moment, and a force due to the knee moment, M′ and knee-force, F′ as shown in Fig. 7. The knee-moment and force can be calculated from the values of linear momentum (Eq. (20)), and angular momentum (Eq. (21)) of the biped links above knee joint. PRBM of initially curved beam is shown in Fig. 8. The compliant link is divided into two rigid links connected with a pin joint and a torsion spring at the joint without any actuators. Hence the compliant-link biped with PRBM has two more passive DoFs (in between the knee and ankle joints of both the legs) and the total degree of freedom is 10. The PRBM link lengths are γl_c and $(1-\gamma)l_c$ (where γ is the characteristics radius factor). For small deflection the value of γ is found to be 0.85. The torsional spring constant K_i ($i = 1, 2$ from Eq. (22)), for the torsional spring can be found by,

$$K_i = \gamma K_\Theta \frac{EI}{l_c} \tag{25}$$

where K_Θ is the stiffness coefficient, E is Young's modulus of the material (Aluminium, 70 GPa), and I is the area moment of inertia of the compliant link. For calculating bending due to both force and moment loading of compliant link, the end deflection, first Θ_i is calculated only for moment loading then the force loading is applied to the initially curved beam [17]. The curvature, κ_i, of the PRBM beam due to only moment loading, M' is found by,

$$\kappa_i = \frac{M' l_c}{EI} \tag{26}$$

and equivalent radius of curvature (R_i) is,

$$R_i = \frac{EI}{M' l_c}. \tag{27}$$

From the curvature and length of the beam, deflections in longitudinal and transverse direction (a_i and b_i respectively) are derived. The end-angle of the pseudo-rigid body, Θ_i, due to moment is found by,

$$\Theta_i = \tan^{-1}\left(\frac{b_i}{a_i - l_c(1-\gamma)}\right). \tag{28}$$

For accurately representing the end-point position of the initially curved compliant link, the length of the PRBM link is given by, ρl_c. The value of ρ can be calculated as,

$$\rho = \left\{\left[\frac{a_i}{l_c} - (1-\gamma)\right]^2 + \left(\frac{b_i}{l_c}\right)^2\right\}^{1/2}. \tag{29}$$

The final deflection angle, Θ due to applied force, F' to this initially curved link is calculated as,

$$\Theta = \frac{(\alpha^2)_t}{K_\Theta} \tag{30}$$

where $(\alpha^2)_t = F_t \times l_c^2/EI$ and F_t is the transverse component of the force F'. The deflection path of the beam end is approximated by,

$$\frac{a}{l_c} = 1 - \gamma + \rho.\cos\Theta$$
$$\frac{b}{l_c} = \rho.\sin\Theta \tag{31}$$

where 'a' and 'b' are the final deflection in longitudinal and transverse direction respectively. Then these deflections are used to find the compliant link biped trajectory.

6. Simulation and results

The simulation for finding optimum trajectory for compliant biped is done in Matlab. The simulation steps are—

- A hip trajectory is generated with respect to the stance-leg ankle and a swing-ankle trajectory is generated with respect to the hip joint.
- Inverse kinematics of the rigid biped is done to find the joint angles.
- Knee moment (M′) and force (F′) are calculated.
- Compliant link position displacements (a & b) and angular deflection (Θ) are calculated.
- Rest of the joint angles of the compliant biped are calculated by inverse kinematics.
- Correction of the other joint angles due to the deflections is done.
- Optimization is done to find the foot trajectory with minimum work done satisfying ZMP criteria for balance.

To generate spline trajectories of the hip link and swing-leg ankle, the input parameter values are side tilt angle, θ_1, X and Z-coordinates of the origin of swing ankle, O_{x_7} and O_{z_7} respectively, height of hip-link centre, H_z and amplitude of the sinusoidal path of hip motion in the Z-direction a_{H_z}. The limits of these input parameters are given as input to the GA function in Matlab, as shown in Table 5. To run the GA program, the step-length (L_{step}), step-time (t_c) are kept constant.

Table 5
Input parameters.

Parameter	Upper limit	Lower limit
$\theta_1(t_m)$	−5°	−15°
$\theta_1(t_{d_1})$ & $\theta_1(t_{d_2})$	−3°	−12°
$O_{z_7}(t_m)$	20 mm	15 mm
$O_{z_7}(t_a)$	30 mm	22 mm
$O_{z_7}(t_b)$	1 mm	0 mm
$O_{x_7}(t_a)$	5 mm	1 mm
$O_{x_7}(t_b)$	5 mm	1 mm
a_{H_z}	5 mm	1 mm
H_Z	210 mm	180 mm

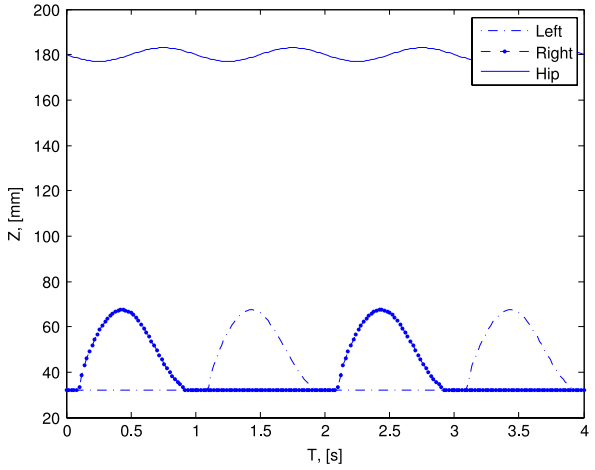

Fig. 9. Hip and ankle trajectory in Z-coordinate vs. time.

6.1. Spline trajectory generation

The spline trajectories are generated for single step with step time, $t_c = 1$ s and step length, $L_{step} = 0.1$ m. In Figs. 9–11, four consecutive steps of gait trajectories are shown for Z, X coordinates and tilt-angle (θ_1 and θ_8). Hip trajectory is defined with sinusoidal curve in the sagittal plane, whose average height is, H_z and amplitude, a_{H_z} (Fig. 9). Swing-leg ankle trajectory is generated with values of O_{z_7} and O_{x_7}. An in-build 3rd order spline generation function in Matlab is used to generate clamped spline to keep end slope values at t_0 and t_c to zero. Side-tilt angle trajectory, θ_1, is also generated with the clamped end spline curve for zero slope at the ends (Fig. 11). Five points for generating the X-trajectory of hip centre, X_H, taken are, $[0, L_{step}/5, L_{step}/2, 4L_{step}/5, L_{step}]$, (Fig. 10). The Y motion of hip centre is dependent upon the side tilt angle. The stance-leg is fixed on the ground, so there is no X or Z direction movement of the stance ankle.

6.2. Optimization

GA is a powerful tool to find optimal biped gaits. Genetic algorithms are known to be efficient and robust in searching for a global solution in optimization [27]. Genetic algorithms are used in many optimization problems for the reasons that they are robust to ill-condition in the optimization function and that they can find global solutions. GA is utilized for bipedal gait generation by minimizing the ZMP error. GA-based path planning produces smooth bipedal movements [28]. The gradient-based method requires computation of gradient that is difficult in the case of Lagrange–Euler dynamic equations used in this work.

GA is used to find the optimum trajectory for minimum work done in a walking step for both rigid and compliant-link bipeds. GA simulation is run on an Intel Core2Duo CPU, E7300, 2.66 GHz processor with 4 GB RAM computer. The simulation is started without

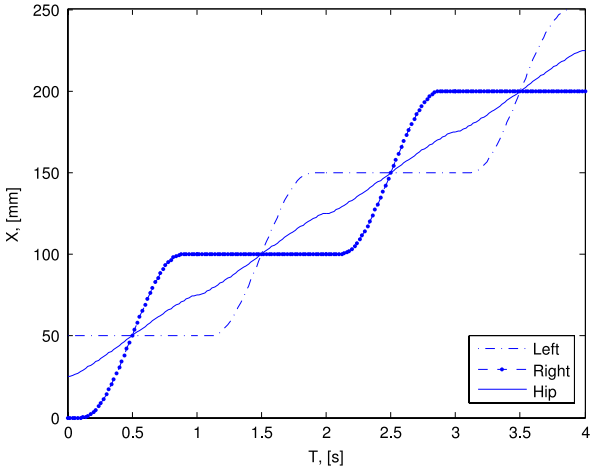

Fig. 10. Hip and ankle trajectory in X-coordinate vs. time.

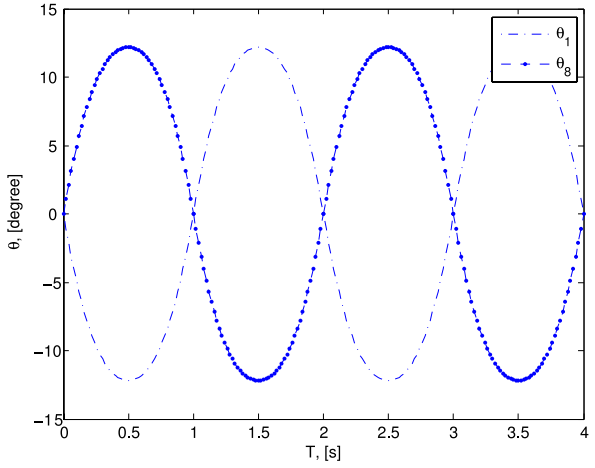

Fig. 11. Side-tilt angle of ankle joints vs. time.

any seed solution and it took around 3 h for each run. Different gait patterns are generated for the biped by varying input parameters. For each of these gait patterns, total work done by the joint motors will be different. GA parameters taken for the simulation are, population size is 20, maximum number of iteration is 1000, crossover probability is 0.9 and mutation probability is 0.05. For each constraint violation a very high value of penalty, 10^7, is added to the objective function. The objective function is,

$$\text{Work done} + \text{penalty} = \text{W} + 10^7 \times n_{cv} \tag{32}$$

where, work done, $W = W_R$, for rigid biped and $W = W_C$, for compliant biped and n_{cv} is the number of times constraint conditions are violated in a single GA simulation.

6.3. Simulation results

From inverse kinematics the joint angle trajectories for rigid biped are found. The angle trajectories in Fig. 12 are generated using an average hip height of 210 mm and step length 100 mm. It can be seen from the figure that the angles vary very smoothly within a single step from one phase to another. The biped continuous gait generated with these angles for multiple steps is shown in Fig. 13.

Joint torques for rigid-link biped are sown in Fig. 14. The torque diagram shows different behaviour in three different phases of walking step. In the first double supported phase, DSP_1 ($t_0 \leq t \leq t_{d_1}$) torque at joint 1, 2 and 4 are having higher values compared to other joints. Although the value of τ_1 and τ_2 are decreasing at

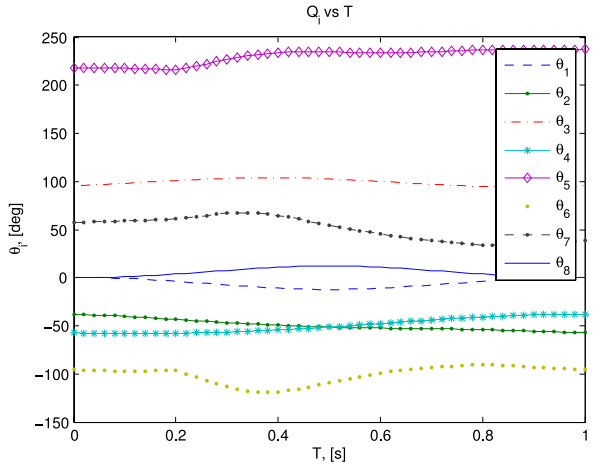

Fig. 12. Variation of angles during a step.

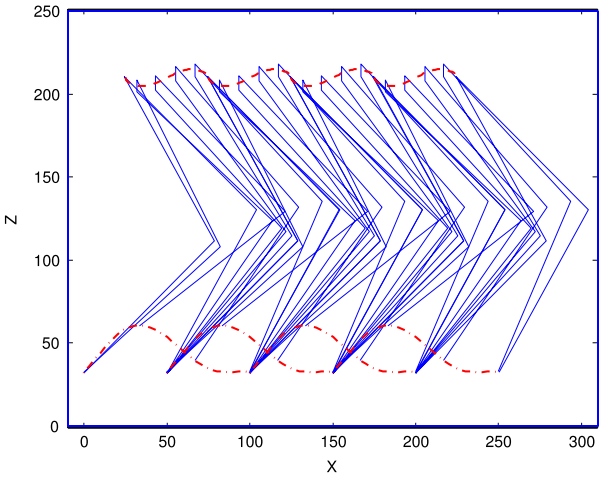

Fig. 13. Multi-step simulation of the rigid-biped.

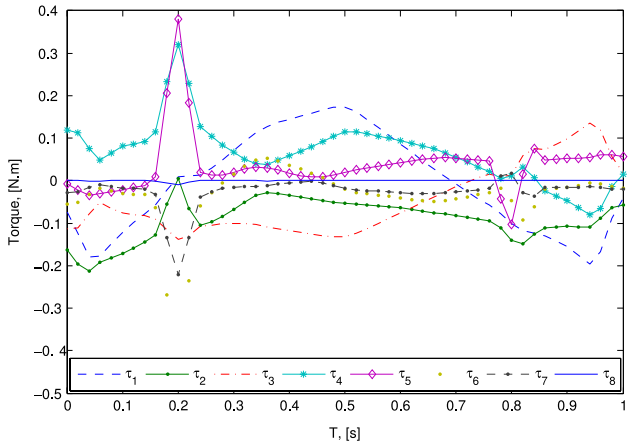

Fig. 14. Rigid-link biped joint torques vs. time.

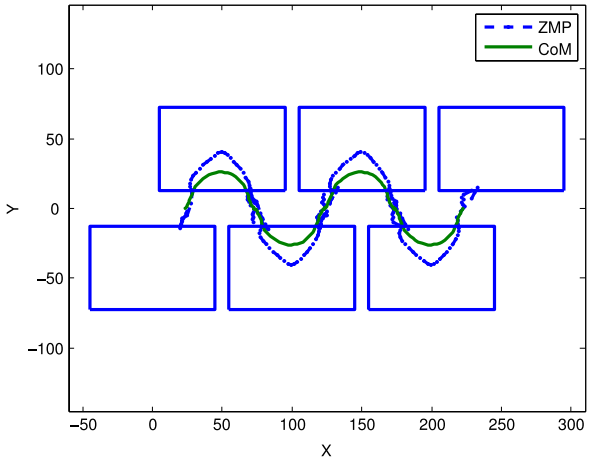

Fig. 15. ZMP CoM for rigid biped.

the end of DSP_1, torque at stance-leg hip joint (τ_4) is increasing as the whole body load is shifting to the stance-leg. The swing-leg hip joint torque (τ_5) is also showing a sudden jerk at t_{d_1}. During SSP ($t_{d_1} < t < t_{d_2}$) the stance-leg ankle roll (τ_1) and knee joint (τ_3) is having a high torque value. Stance-leg hip joint torque is also high. In the beginning of SSP, torque at stance ankle pitch (τ_2) is low but slowly increasing at the end of SSP. During the third phase of the gait, DSP_2 ($t_{d_2} < t \leq t_c$), τ_1, τ_2 and τ_3 are having higher values compared to other joint torques.

The ZMP and CoM for rigid biped are shown in Fig. 15 for 4 steps. It is found that the sudden jerky variation in joint torques also affects the ZMP trajectory during the phase change. The jerks take place due to sudden change in load from one leg to another that causes sudden deflections in the compliant leg.

For compliant-link biped we have done simulation with the same hip height configuration as in the rigid-link biped with 4 different compliant link thickness. We are compensating the knee and ankle joint angles according to the deflection in the compliant link, to keep the lower trunk upright. But in this way the balance could not be established during walking. So, we ran GA optimization program for compliant biped separately, keeping other parameters same and found the compliant walking gait for balance and minimum work done. In Table 6 work done for both rigid biped and compliant-link biped (with different compliant link thickness) are shown. Very little variation in work is noticed for changing compliant link thickness. But for increasing average hip-height, H_z, the work done increases. For rigid biped also the increase of work with

Table 6
Work done by compliant and rigid biped with $t_{d_1} = t_{d_2} = 10/50$, for different hip height, H_z, for walking.

H_z (mm)	Work (J × 10^{-1})				
	Compliant				Rigid
	0.5 (mm)	1.0 (mm)	1.5 (mm)	2 (mm)	
180	1.712	1.552	1.572	1.571	1.842
190	1.596	1.584	1.632	1.623	1.851
200	2.042	1.668	1.734	1.726	1.914
210	2.473	2.168	1.941	1.927	2.103

H_z is seen. In comparison with rigid biped the compliant-link biped walking takes more effort.

Deflections in compliant link in transverse and axial directions ('a' and 'b' respectively) are shown in Fig. 16. Both the deflections start from zero value then suddenly start increasing at the end of DSP_1 and vary smoothly in SSP. Then these values go towards zero at the end of the step.

Joint torques of compliant-link biped are shown in Fig. 17. In this diagram also three distinct phases can be noticed. In the DSP_1, the torque values at all the stance-leg joint are higher compared to swing-leg. At the end of DSP_1 the swing-leg ankle roll (τ_1), knee (τ_4) and hip (τ_5) joint have a jerk in torque diagram. Then in SSP, the stance-leg ankle roll torque (τ_1) is starting from very low value, then at the middle of the SSP it gradually increases to the highest value and at the end of SSP it again goes to zero. Swing leg ankle pitch torque (τ_9) is having high values at the beginning of SSP but reduces at the end of SSP and τ_2 and τ_7 are increasing at the end

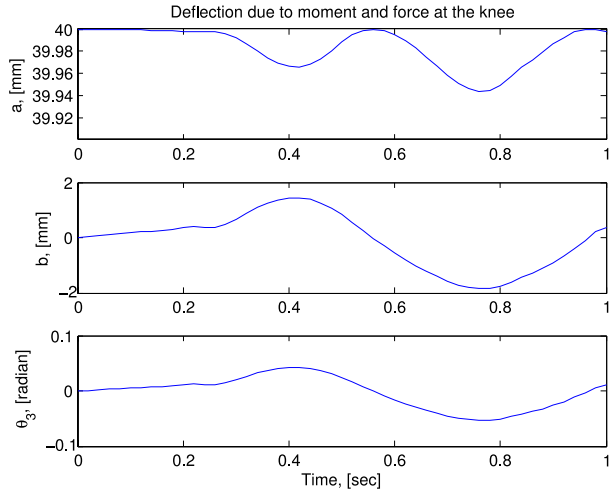

Fig. 16. Deflection of compliant link due to walking motion during one step.

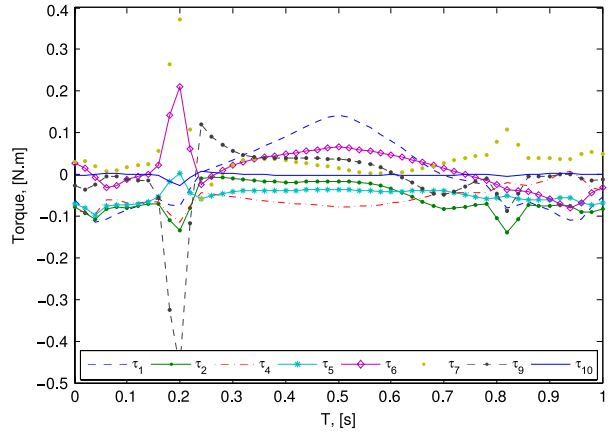

Fig. 17. Compliant-link biped joint torques vs. time.

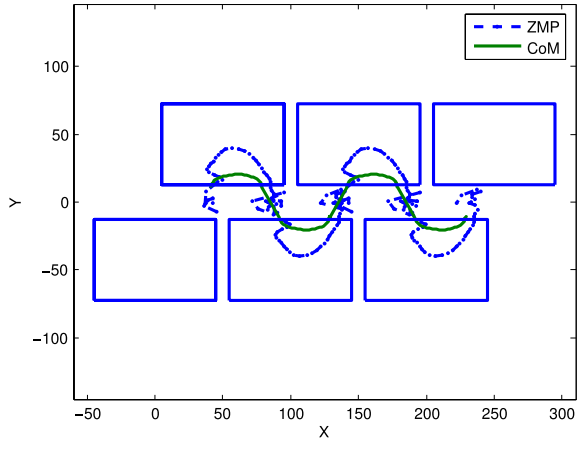

Fig. 18. ZMP CoM for compliant biped, $L_{step} = 100$ mm.

of SSP. During the third phase, DSP_2 except swing leg ankle joints and stance knee joint all other joint are having high values.

The compliant biped ZMP and CoM for multiple steps are shown in Fig. 18. It can be seen from the figure that although the compliant biped walking is stable (i.e. ZMP is inside the feet support polygon all the time) but at the end of the DSP_1 the biped has a backward force acting. So, the lower trunk goes slightly backward during every step.

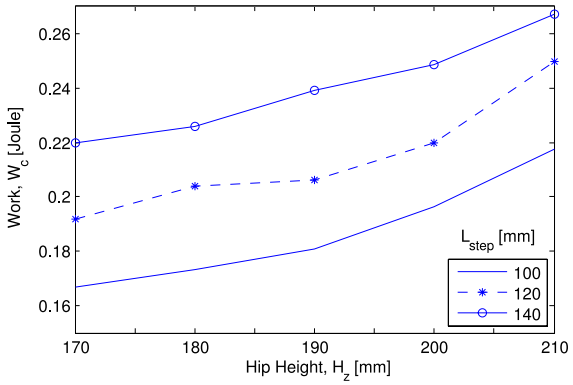

Fig. 19. Variation of work with different H_z and L_{step} for compliant link with thickness 1 mm.

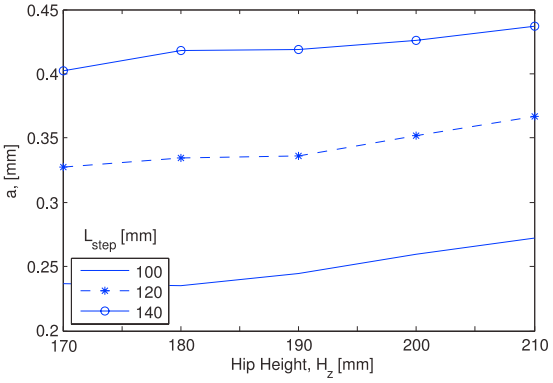

Fig. 20. Variation of deflection 'a' with different H_z and L_{step} for compliant link with thickness 1 mm.

For the compliant biped the variation of work is compared with both hip height and three different step lengths, ($L_{step} = 100$, 120 and 140 mm) as shown in Fig. 19. The highest step length is taken as 140 mm, which is bound by the H_z^{max} constraints of hip height. The work done is higher for higher hip height for all step lengths. But for decreasing hip heights (170–180 mm) the work is increasing a little for $L_{step} = 140$ mm. Work is almost constant for lower step length with decreasing hip height. We tried to find a correlation of work with the vibration amplitude of the compliant link. The plot of variation of 'a' with various L_{step} and H_z is shown in Fig. 20. It shows with increasing step length and hip height '*a*' got increased almost linearly.

6.4. Experimental results

The Biped has been developed using the Bioloid Premium kit [18] with Dynamixel motors (AX-12A) having 1.5 Nm of stall-torque, no-load speed is 59 RPM and minimum control angle is about 0.29°. The controller is CM-530 which has the CPU 'ARM Cortex STM32F103RE'. For developing the compliant-link biped we changed the connector between the knee joint and ankle joint with 'C'-shaped compliant links made of aluminium sheets of thickness 1 mm. The angle values from the simulation results are used to create two consecutive continuous steps of walking gait and then converted to the corresponding motor angle values. These angle values are then given to the motor controller by the Roboplus software [18].

Video of the rigid-body and compliant-link biped walk were recorded at a frame rate of 50 frames/second. Then these frames are extracted from the videos with OpenCV for capturing trajectory values. Few frames taken from a single step of walking for both bipeds are shown in Fig. 21(a) and (b) respectively. It can be

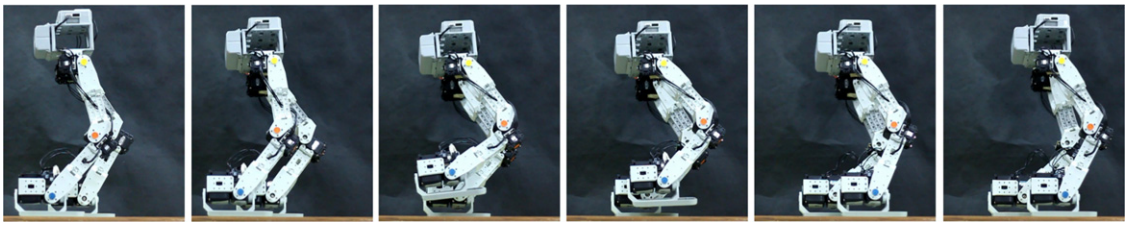

(a) Rigid-link biped trajectory.

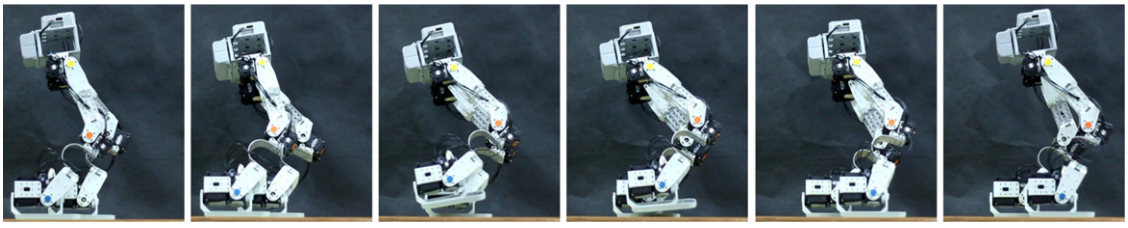

(b) Compliant-link biped trajectory.

Fig. 21. Frame extracted from video of biped walking for a single step. (For interpretation of the references to colour in this figure legend, the reader is referred to the web version of this article.)

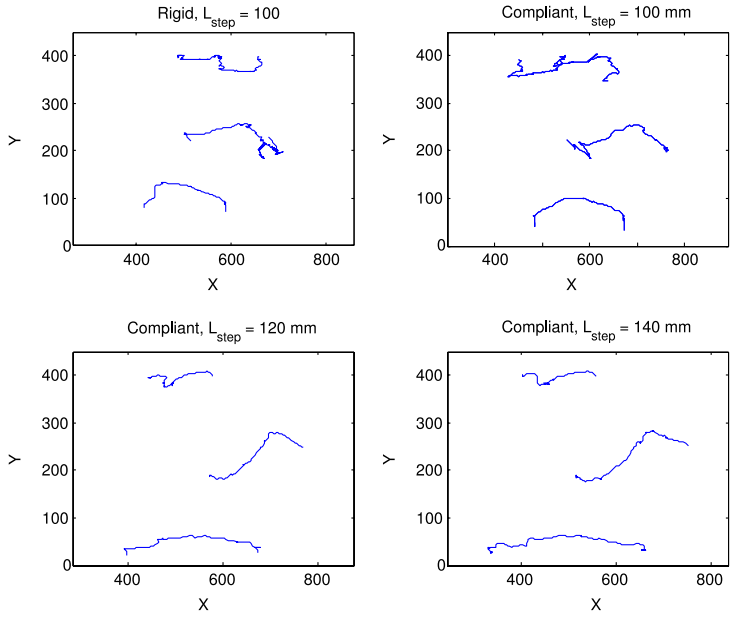

Fig. 22. Trajectory of rigid and compliant biped walking in image coordinates.

seen from the figures that during the SSP the lower trunk of the compliant-link biped is leaning backward compared to the rigid-body biped. Markers are attached at the ankle, knee, and hip motor axes with different colours. The coordinates of these markers are detected on each frame extracted through OpenCV. Then they are taken together to generate the trajectory as shown in Fig. 22. The rigid biped is following the exact step length of 100 mm as given in input. At the beginning phase of the step (DSP_1) for hip joint of rigid biped a loop is formed which is due to the side tilting motion of the biped and backlash at the joints. Also during the transition from SSP to DSP_2 there are some jerks visible due to the landing of swing foot. The hip and swing foot trajectories are roughly following the simulation pattern. The compliant biped hip trajectory during DSP_1 has an initial dip as the compliant leg deflects and the body moves backwards as soon as biped lifts one leg. During SSP also the movement is wobbly and the swing foot trajectory is also deviating from simulation trajectories. At the end of the SSP the compliant biped is having some jerky movements in hip motion due to the touch-down of the swing foot. For higher values of step length (120 and 140 mm) of compliant biped the foot trajectory is lower than the desired input trajectories. Hence, an early touchdown of the swing foot occurs resulting in a jerk near the terminal swing phase.

7. Conclusion

A compliant link with bending deflection is attached to a 8-DoF rigid-body biped by replacing the link between both the knee and ankle joints. Continuous walking gait is generated for both rigid and compliant-link bipeds and the optimization is carried out to generate a stable walking trajectory and minimize the work done. An experiment is carried out with the developed biped model to see the actual trajectories of both the bipeds. Although the simulation results show that the variations of angles are very smooth but in experiments we have seen vibrations in the motion of the compliant biped. Experiments with the variation of step lengths are carried out.

References

[1] C. Chevallereau, G. Bessonnet, G. Abba, Y. Aoustin, Bipedal Robots: Modeling, Design and Walking Synthesis, Wiley.com, 2010, http://dx.doi.org/10.1002/9780470611623.

[2] M. Hirose, K. Ogawa, Honda humanoid robots development, Phil. Trans. R. Soc. A 365 (2007) 11–19. http://dx.doi.org/10.1098/rsta.2006.1917.

[3] S. Kajita, K. Tani, Experimental study of biped dynamic walking, IEEE Control Syst. 16 (1) (1996) 13–19. http://dx.doi.org/10.1109/37.482132.

[4] C.-L. Shih, Gait synthesis for a biped robot, Robotica 15 (6) (1997) 599–607. http://dx.doi.org/10.1017/S0263574797000726.

[5] M.J. Er, W.S. Khor, Z. Tang, Humanoid gait synthesis using trajectory plot and relative-ZMP (R-ZMP) concept, in: 17th IFAC World Congress, 2008, pp. 2394–2399. http://dx.doi.org/10.3182/20080706-5-KR-1001.00404.

[6] S. Dalibard, et al., Dynamic walking and whole-body motion planning for humanoid robots: an integrated approach, Int. J. Robot. Res. 32 (9–10) (2013) 1089–1103. http://dx.doi.org/10.1177/0278364913481250.

[7] D. Goswami, V. Prahlad, P.D. Kien, Genetic algorithm-based optimal bipedal walking gait synthesis considering tradeoff between stability margin and speed, Robotica 27 (03) (2009) 355–365. http://dx.doi.org/10.1017/S026357470800475X.

[8] R.M. Alexander, Three uses for springs in legged locomotion, Int. J. Robot. Res. 9 (2) (1990) 53–61. http://dx.doi.org/10.1177/027836499000900205.

[9] Z. Li, N.G. Tsagarakis, D.G. Caldwell, Walking pattern generation for a humanoid robot with compliant joints, Auton. Robots 35 (1) (2013) 1–14. http://dx.doi.org/10.1007/s10514-013-9330-7.

[10] T. Schauß, M. Scheint, M. Sobotka, W. Seiberl, M. Buss, Effects of compliant ankles on bipedal locomotion, in: Robotics and Automation, IEEE International Conference on, IEEE, 2009, pp. 2761–2766. http://dx.doi.org/10.1109/ROBOT.2009.5152526.

[11] H. Geyer, A. Seyfarth, R. Blickhan, Compliant leg behaviour explains basic dynamics of walking and running, in: Proceedings of the Royal Society B: Biological Sciences, Vol. 273, The Royal Society, 2006, pp. 2861–2867. http://dx.doi.org/10.1098/rspb.2006.3637.

[12] F. Iida, J. Rummel, A. Seyfarth, Bipedal walking and running with spring-like biarticular muscles, J. Biomech. 41 (3) (2008) 656–667. http://dx.doi.org/10.1016/j.jbiomech.2007.09.033.

[13] D. Owaki, H. Fukuda, A. Ishiguro, Adaptive bipedal walking through sensory-motor coordination yielded from soft deformable feet, in: International Conference on Intelligent Robots and Systems, Vilamoura, Algarve, Portugal, IEEE/RSJ, 2012, pp. 4257–4263. http://dx.doi.org/10.1109/IROS.2012.6385894.

[14] I. Mizuuchi, Y. Nakanishi, Y. Sodeyama, Y. Namiki, T. Nishino, N. Muramatsu, J. Urata, K. Hongo, T. Yoshikai, M. Inaba, An advanced musculoskeletal humanoid Kojiro, in: Humanoid Robots, 7th IEEE-RAS International Conference on, IEEE, 2007, pp. 294–299. http://dx.doi.org/10.1109/ICHR.2007.4813883.

[15] R. Niiyama, S. Nishikawa, Y. Kuniyoshi, Athlete robot with applied human muscle activation patterns for bipedal running, in: Humanoid Robots (Humanoids), 10th IEEE-RAS International Conference on, IEEE, 2010, pp. 498–503. http://dx.doi.org/10.1109/ICHR.2010.5686316.

[16] L.L. Howell, Compliant Mechanisms, Wiley-Interscience, 2001.

[17] A. Saxena, S. Kramer, A simple and accurate method for determining large deflections in compliant mechanisms subjected to end forces and moments, J. Mech. Des. 120 (1998) 392–400. http://dx.doi.org/10.1115/1.2829164.

[18] Robotis Website. http://www.robotis.com/xe/.

[19] K.S. Fu, R.C. Gonzalez, C. Lee, Robotics: Control, Sensing, Vision and Intelligence, McGraw-Hill Book, 1987.

[20] A. Ghosal, Robotics: Fundamental Concepts and Analysis, Oxford University Press, 2006.

[21] B.C. Fabien, Analytical System Dynamics, Springer, 2009.

[22] Y.-Q. Yu, L.L. Howell, C. Lusk, Y. Yue, M.-G. He, Dynamic modeling of compliant mechanisms based on the pseudo-rigid-body model, J. Mech. Des. 127 (2005) 760–765. http://dx.doi.org/10.1115/1.1900750.

[23] M.H. Korayem, H.N. Rahimi, Nonlinear dynamic analysis for elastic robotic arms, Front. Mech. Eng. 6 (2) (2011) 219–228. http://dx.doi.org/10.1007/s11465-011-0218-y.

[24] M. Vukobratović, B. Borovac, Zero-moment point-thirty five years of its life, Int. J. Humanoid Rob. 1 (01) (2004) 157–173. http://dx.doi.org/10.1142/S0219843604000083.

[25] P. Sardain, G. Bessonnet, Forces acting on a biped robot. Center of pressure-zero moment point, IEEE Trans. Syst. Man Cybern. A 34 (5) (2004) 630–637. http://dx.doi.org/10.1109/TSMCA.2004.832811.

[26] L. Howell, A. Midha, T. Norton, Evaluation of equivalent spring stiffness for use in a pseudo-rigid-body model of large-deflection compliant mechanisms, J. Mech. Des. 118 (1996) 126–131. http://dx.doi.org/10.1115/1.2826843.

[27] G. Capi, S.-i. Kaneko, K. Mitobe, L. Barolli, Y. Nasu, Optimal trajectory generation for a prismatic joint biped robot using genetic algorithms, Robot. Auton. Syst. 38 (2) (2002) 119–128. http://dx.doi.org/10.1016/S0921-8890(01)00177-4.

[28] S.-H. Choi, Y.-H. Choi, J.-G. Kim, Optimal walking trajectory generation for a biped robot using genetic algorithm, in: Intelligent Robots and Systems, 1999. IROS'99. Proceedings, 1999 IEEE/RSJ International Conference on, Vol. 3, 1999, pp. 1456–1461. http://dx.doi.org/10.1109/IROS.1999.811684.

Abhishek Sarkar received his B.Tech. Degree in Mechanical Engineering from Jalpaiguri Govt. Engineering College, India, in 2006 and M.Engg. degree in Production Engineering from the Jadavpur University, India, in 2009. He joined Ph.D. in Mechanical Engineering Department at Indian Institute of Technology, Kanpur, India, in 2010. He is currently working on biped robots, compliant mechanism.

Ashish Dutta obtained his *Ph.D.* in Systems Engineering from Akita University, Japan. From 1994 to 2000 he was with the Bhabha Atomic Research Center (India) where he worked on telemanipulator design and control for nuclear applications. Since 2002 he is with the department of mechanical engineering in the Indian Institute of Technology Kanpur, India. Briefly, he was also an assistant professor in Nagoya University, Japan, from 2006 to 2007 in the department of Mechanical Science and Engineering. His research interests are in the areas of humanoid robotics, micro sensors and actuators, intelligent control systems and rehabilitation engineering.